Biophysical Chemistry 149 (2010) 83–91

Contents lists available at ScienceDirect

Biophysical Chemistry

journal homepage: http://www.elsevier.com/locate/biophyschem

Allowance for the effect of protein charge in the characterization of nonideal solute self-association by sedimentation equilibrium

David J. Scott [a], Peter R. Wills [b], Donald J. Winzor [c,*]

[a] National Center for Macromolecular Hydrodynamics, University of Nottingham School of Biosciences, Sutton Bonington LE12 5RD, United Kingdom
[b] 37 Fairlands Avenue, Waterview, Auckland 1026, New Zealand
[c] School of Chemistry and Molecular Biosciences, University of Queensland, Brisbane, Queensland 4072, Australia

ARTICLE INFO

Article history:
Received 25 March 2010
Accepted 3 April 2010
Available online 4 May 2010

Keywords:
Sedimentation equilibrium
Protein self-association
Scaled particle theory
Thermodynamic non-ideality

ABSTRACT

This theoretical investigation explores the use of statistical–mechanical approaches to characterize the reversible tetramerization of a protein monomer with the size and charge characteristics of serum albumin under conditions where consideration of nearest-neighbor interactions suffices to describe effects of thermodynamic non-ideality. Such analysis of simulated sedimentation equilibrium distributions points to the adequacy of both the scaled particle theory and potential-of-mean-force methods for determining the self-association constant. Although the latter method usually entails the assignment of a magnitude to monomer net charge, this requirement can be obviated to some extent by repeating the analysis for a range of monomer charges and identifying the most appropriate value as that associated with a minimum in the sum-of-squares-of-residuals (SSR) of the best-fit descriptions of the sedimentation equilibrium distribution. Reasonable estimates of the association constant are usually obtained from corresponding analyses of the same sedimentation equilibrium distributions with activity coefficients obtained by scaled particle theory, an approach which also involves the identification of parameters on the basis of a minimum in SSR. However, the value of monomer charge determined must be regarded as a curve-fitting parameter rather than a true measure of monomer charge. Similar qualifications are shown to prevail in the scaled particle theory approach, which also involves the identification of parameters (the effective monomer volume and the polymer/monomer volume ratio) on the basis of a minimum in SSR. We therefore recommend discontinuation of the practice whereby quite precise distinction between modes of self-association has been attempted on the grounds of the physical credibility of the magnitudes of these additional curve-fitting parameters.

© 2010 Elsevier B.V. All rights reserved.

1. Introduction

The existence of interactions between clusters of molecules in a solution of a single solute necessitates description of the thermodynamic activity (effective concentration) as a product of the actual concentration and an activity coefficient that takes into account the consequences of non-ideality arising from those interactions. Indeed, the same situation necessarily applies to a solute undergoing reversible self-association on the grounds of its designation as a single thermodynamic component. However, custom dictates the consideration of clusters arising from short-range contact forces as separately identifiable molecular species, whereupon the number of nominal "components" is increased to incorporate the different oligomeric states of the single solute. In terms of this notional concept the clusters reflecting short-range dispersion forces and attractions between molecules due to specific group interactions (i.e., "associative forces") are described by the product of an association constant and the thermodynamic activity of monomer raised to the appropriate power. On the other hand, clusters reflecting excluded volume forces and the relatively long-range forces due to the presence of ionically-screened electrostatic fields around molecules (i.e., "non-associative forces") are attributed to thermodynamic non-ideality that is incorporated into an activity coefficient for each oligomeric state of the solute.

A recent theoretical investigation of methods for characterizing nonideal solute self-association by sedimentation equilibrium [1] has demonstrated the need to replace procedures based on the Adams–Fujita assumption [2] by analyses that incorporate descriptions of thermodynamic non-ideality based on the statistical–mechanical concept of the potential-of-mean-force. Of those methods, the most direct entails an adaptation of the Hill–Chen single-solute approach

* Corresponding author. Fax: +61 7 3365 4699.
E-mail address: d.winzor@uq.edu.au (D.J. Winzor).

0301-4622/$ – see front matter © 2010 Elsevier B.V. All rights reserved.
doi:10.1016/j.bpc.2010.04.003

[3] wherein total solute concentration is expressed as a virial expansion in the thermodynamic activity of monomer [4–6]. Consideration of solute self-association as a multi-solute system necessitates the introduction of a composition-dependent activity coefficient for each species and hence reliance upon an iterative approach to obtain the self-association constant(s) [7,8]. This process of iteration is also central to an alternative statistical–mechanical approach in which the activity coefficients are defined on the basis of scaled particle theory [9–11]. Here, each molecule is represented by a sphere with radius scaled to take account of its mass: hence a dimer is considered to have a radius $2^{1/3}$ times that of the monomer. All three statistical–mechanical approaches have been shown [1] to return essentially identical estimates of the dimerization constant from simulated sedimentation equilibrium distributions with an upper concentration limit of 10 g/L (10 mg/mL).

The current study extends our earlier investigation [1] by examining situations in which the solute (protein) not only bears net charge, but also associates beyond a dimer. The combination of these two considerations precludes general use of any single-solute approach [3–6] because of the difficulty of obtaining expressions for the coefficients of the quartic and higher-order terms in the virial expansion of total solute concentration as a function of monomer activity. Attention is thus, of necessity, centered on the two iterative approaches involving composition-dependent activity coefficients. Despite the consequent restriction of non-ideality considerations to effects of nearest-neighbor interactions, it should be noted that the second virial coefficient for tetramer self-interaction covers the equivalent of a term in monomer activity raised to the eighth power in the single-solute approach. In that sense the single-solute method for characterizing a monomer–dimer equilibrium may be considered to suffer from the disadvantage of requiring a description of the virial expansion correct to the quartic power in monomer activity in order to accommodate the nearest-neighbor interactions that are covered by second virial coefficient terms in the two-solute approach.

A limitation of scaled particle theory (SPT) for the quantification of non-ideality is its inability directly to account for effects of electrostatic repulsion. This deficiency can be theoretically overcome for a single non-associating solute by increasing the effective size of the sphere to account for charge–charge repulsive effects [12]. The assumption is then made that the effects of electrostatic repulsion on protein–protein self-association can be handled in a similar manner [11,13–16]. To date, however, the only attempts to justify this assumption have entailed demonstrations that the thermodynamic non-ideality of a *mixture* of two non-interacting solutes is described by the *sum* of non-ideality predicted by scaled particle theory and the effective sizes of the two solutes inferred from *separate* studies of the individual solutes [16,17]. Unfortunately, that finding does not comment on the situation pertaining to a self-associating system, where the co-existing equilibrium of monomer and oligomer species prevents deduction of their effective sizes from studies of each in isolation.

In this investigation we compare the different approaches for characterizing the self-association of a charged protein by analyzing precisely simulated sedimentation equilibrium distributions for monomer–tetramer systems based on protein monomers the size of serum albumin. The major outcome of this exercise is a demonstration of the need for caution in assigning significance to magnitudes of the statistical fitting parameters emanating from either sort of analysis, a proviso that renders questionable their use [1–3,13–16] to distinguish between different models of self-association.

2. Theoretical considerations

In the two-solute model of protein self-association ($nA \leftrightharpoons P$) the molar thermodynamic activity of each species (z_i) is expressed as the product of its molar concentration (C_i) and an activity coefficient (γ_i), whereupon the molar thermodynamic association constant (K_n) is defined by the relationship

$$K_n = \frac{z_P}{z_A^n} = \frac{C_P\gamma_P}{(C_A\gamma_A)^n}. \tag{1a}$$

Alternatively, description of the thermodynamic activity coefficients on a weight–concentration basis as the product of z_i and molar mass M_i, leads to the expression

$$X_n = \frac{M_P z_P}{(M_A z_A)^n} = \frac{c_P\gamma_P}{(c_A\gamma_A)^n} \tag{1b}$$

where $X_n = nK_n/M_A^{n-1}$ is the weight–concentration counterpart of K_n. Evaluation of a meaningful equilibrium constant is thus dependent upon the assignment of appropriate magnitudes to the activity coefficients for both the monomer and polymer species.

2.1. Expressions for activity coefficients

Subject to the proviso that effects of nearest-neighbor interactions suffice to describe the thermodynamic non-ideality, the activity coefficients for monomer (γ_A) and polymer (γ_P) are defined on the statistical–mechanical basis of the potential-of-mean-force between molecules as [18,19]:

$$\gamma_A = \exp\left(2B_{AA}C_A + B_{AP}C_P\right) = \exp\left(2\frac{B_{AA}}{M_A}c_A + \frac{B_{AP}}{M_P}c_P\right) \tag{2a}$$

$$\gamma_P = \exp\left(2B_{PP}C_P + B_{AP}C_A\right) = \exp\left(2\frac{B_{PP}}{M_P}c_P + \frac{B_{AP}}{M_A}c_A\right). \tag{2b}$$

B_{AA} and B_{PP} are osmotic second virial coefficients for self-interaction of monomer and polymer respectively, whereas B_{AP} refers to the corresponding second virial coefficient reflecting physical interaction between monomer and polymer. Furthermore, magnitudes of the three virial coefficients may be calculated by assuming that both species are spheres (equivalent radius R for the hydrated molecular species) with net charge Z spread uniformly over their surfaces, in which case advantage can usually be taken of the approximate expressions [6,20,21]:

$$B_{ij} = \frac{2\left(2-\delta_{ij}\right)\pi L\left(R_i+R_j\right)^3}{3} + \frac{\left(2-\delta_{ij}\right)Z_iZ_j\left(1+\kappa R_i+\kappa R_j\right)}{4I_M(1+\kappa R_i)\left(1+\kappa R_j\right)} - \frac{1000\left(2-\delta_{ij}\right)Z_i^2Z_j^2\kappa^3}{128\pi LI_M^2(1+\kappa R_i)^2\left(1+\kappa R_j\right)^2} + \ldots \tag{3}$$

where δ_{ij} is the Kronecker delta (equal to unity if $i=j$, otherwise zero) and the magnitude in cm^{-1} of κ, the Debye inverse screening length, is deduced from the gram–molar magnitude of the ionic strength I_M as $3.27\times10^7\sqrt{I_M}$. The appearance of Avogadro's number (L) in these expressions reflects the conversion of virial coefficients from a molecular to a molar basis (L/mol); and the factor of 1000 in the final term takes into account the implied units of κ^3 (cm^{-3}). For proteins with a reasonably uniform charge distribution the requirement in Eqs. (1a) and (1b) of magnitudes for γ_A and γ_P can thus be met with an acceptable degree of precision by combining measurements of the Stokes radius and net charge of monomer with the concepts of spherical geometry, $R_P = n^{1/3}R_A$, and charge conservation, $Z_P = nZ_A$.

Unfortunately, for highly charged systems the series in Eq. (3) begins to converge far too slowly for reliable estimates of second virial coefficients to be obtained by this means. In the present study we have therefore reverted to the reliable estimation of the virial coefficients

by numerical integration of the equations of which the last two terms of Eq. (3) are the approximate solutions. Specifically, the second virial coefficient (B_{ij}) for interaction between a molecule of species i and one of j is obtained from the expression

$$B_{ij} = \frac{2\left(2-\delta_{ij}\right)\pi L\left(R_i + R_j\right)}{3} - 2\left(2-\delta_{ij}\right)\pi L\int_{R_i+R_j}^{\infty} f_{ij}(x)x^2dx \tag{4a}$$

where the Mayer f-function, $f_{ij}(x)$, is given by

$$f_{ij}(x) = \exp\left[\frac{-u_{ij}(x)}{kT}\right] - 1. \tag{4b}$$

In this expression $u_{ij}(x)$ specifies the potential energy of the two molecules as a function of the center-to-center separation x, and k the Boltzmann constant. For spherical molecules with radii R_i and R_j the energy function is described in terms of the inverse screening length (κ), the dielectric constant of the solvent medium (ε), electronic charge (e) and the net charge of the molecules (Z_i and Z_j) by

$$u_{ij} = \begin{cases} \infty & x < R_i + R_j \\ \dfrac{Z_iZ_je^2\exp\left[-\kappa\left(x-R_i-R_j\right)\right]}{\varepsilon(1+\kappa R_i)\left(1+\kappa R_j\right)x} & x \geq R_i + R_j \end{cases} \tag{4c}$$

or, taking advantage of the relationship between the ionic strength and the inverse screening length

$$\kappa^2 = \frac{8\pi Le^2 I_M}{\varepsilon kT}, \tag{5a}$$

we have

$$\frac{u_{ij}(x)}{kT} = \frac{1000Z_iZ_j\kappa^2\exp\left[-\kappa\left(x-R_i-R_j\right)\right]}{8\pi LI_M(1+\kappa R_i)\left(1+\kappa R_j\right)x} \qquad x \geq R_i + R_j. \tag{5b}$$

For an uncharged protein ($Z_A = Z_P = 0$) the required virial coefficients and hence activity coefficients simply become functions of monomer molar volume, $V_A = 4\pi LR_A^3/3$, a simplification which allows scaled particle theory [9,22] to be used as an alternative statistical–mechanical treatment of thermodynamic non-ideality in terms of excluded volume as the sole contribution to the potential-of-mean-force between molecules. In an attempt to broaden the applicability of scaled particle theory to studies of protein self-association the stance has been taken [11–16] that the additional excluded volume arising from charge–charge repulsion can be accommodated by increasing the effective size of the representative solute species. The activity coefficients of monomer and polymer species are then given by the following expressions [1]:

$$Q\gamma_A = \exp\left\{\begin{array}{l} \left(\frac{1}{Q}\right)\left(\frac{V_A^{\mathrm{eff}}}{M_A}\right)\left[7c_A + \left(\frac{3x^2}{n^{1/3}} + \frac{3x}{n^{2/3}} + \frac{1}{n}\right)(\bar{c}-c_A)\right] \\ + \left(\frac{3}{Q^2}\right)\left(\frac{V_A^{\mathrm{eff}}}{M_A}\right)^2\left[c_A + \frac{x^2(\bar{c}-c_A)}{n^{1/3}}\right] \\ \times\left[\frac{5}{2}c_A + \left(\frac{3x^2}{2n^{1/3}} + \frac{x}{n^{2/3}}\right)(\bar{c}-c_A)\right] \\ + \left(\frac{3}{Q^3}\right)\left(\frac{V_A^{\mathrm{eff}}}{M_A}\right)^3\left[c_A + \frac{x^2(\bar{c}-c_A)}{n^{1/3}}\right]^3 \end{array}\right\} \tag{6a}$$

$$Q\gamma_P = \exp\left\{\begin{array}{l} \left(\frac{1}{Q}\right)\left(\frac{V_A^{\mathrm{eff}}}{M_A}\right)\left[7x^3(\bar{c}-c_A) + \left(3n^{1/3}x + 3n^{2/3}x^2 + nx^3\right)c_A\right] \\ + \left(\frac{3}{Q^2}\right)\left(\frac{V_A^{\mathrm{eff}}}{M_A}\right)^2\left[x^3(\bar{c}-c_A) + n^{1/3}xc_A\right] \\ \times\left[5x^3(\bar{c}-c_A)/2 + \left(3n^{1/3}x/2 + n^{2/3}x^2\right)c_A\right] \\ + \left(\frac{3}{Q^3}\right)\left(\frac{V_A^{\mathrm{eff}}}{M_A}\right)^3\left[x^3(\bar{c}-c_A) + n^{1/3}xc_A\right]^3 \end{array}\right\} \tag{6b}$$

where

$$Q = 1 - \frac{V_A^{\mathrm{eff}}}{M_A}\left[c_A + x^3(\bar{c}-c_A)\right] \tag{6c}$$

and $V_A^{\mathrm{eff}} = 4\pi L(R_A^{\mathrm{eff}})^3$ denotes the effective molar volume of monomer. The effective volume of polymer (V_P^{eff}) is expressed as $nx^3V_A^{\mathrm{eff}}$ to allow for differences between V_P^{eff} and nV_A^{eff} because of charge–charge contributions to both these parameters. In that regard Eqs. (6b) and (6c) effectively duplicate Eqs. (14b) and (14c) of our previous study [1], whereas Eq. (6a) rectifies typographical omissions from the earlier expression for the activity coefficient of monomer.

The essential identity of activity coefficients obtained by this approach for self-associating systems and those emanating from the traditional statistical–mechanical treatment of thermodynamic non-ideality in a two-solute system [Eqs. (2a), (2b) and (3)] has been illustrated recently [1] for dimerization of uncharged systems ($Z_A = Z_P = 0$, $n = 2$, $x = 1$). However, no attempt seems to have been made to test the adequacy or, indeed, validity of Eqs. (6a)–(6c) in situations where the self-associating solute bears net charge ($Z_A \neq 0$, $x \neq 1$).

2.2. Analysis of sedimentation equilibrium distributions reflecting solute self-association

In an experiment conducted at angular velocity ω and absolute temperature T the radial distribution of species i (with molar mass M_i) at sedimentation equilibrium is described by the expression [23,24]

$$z_i(r) = z_i(r_F)\exp\left[M_i(1-\bar{\nu}_i\rho_s)\frac{\omega^2}{2RT}\left(r^2-r_F^2\right)\right] \tag{7}$$

as the relationship between the thermodynamic activity of the species at radial distance r to its value at a selected reference radial position r_F. $\bar{\nu}_i$ is the partial specific volume of the species, ρ_s is the solvent density [25], and R is the universal gas constant. On the grounds that the partial specific volumes of different oligomeric states may reasonably be equated with that ($\bar{\nu}$) of the protein, the concentration distribution of a self-associating protein at sedimentation equilibrium becomes

$$\begin{aligned} \bar{c}(r) &= \frac{M_Az_A(r)}{\gamma_A(r)} + X_n\frac{[M_Az_A(r)]^n}{\gamma_P(r)} \\ &= \frac{M_Az_A(r_F)\psi_A(r)}{\gamma_A(r)} + \frac{X_n[M_Az_A(r_F)\psi_A(r)]^n}{\gamma_P(r)} \end{aligned} \tag{8a}$$

where

$$\psi_A(r) = \exp\left[M_A(1-\bar{\nu}_i\rho_s)\frac{\omega^2}{2RT}\left(r^2-r_F^2\right)\right] \tag{8b}$$

and $\gamma_A(r)$, $\gamma_P(r)$ are the respective activity coefficients of monomer and polymer corresponding to the total weight–concentration of protein at radial distance r.

Magnitudes of the thermodynamic activity of monomer at the reference radial distance, $z_A(r_F)$, and the association constant, X_n, are fixed parameters that can, in principle, be obtained by nonlinear curve-fitting of the $[\psi_A(r),\bar{c}(r)\gamma_A(r),\gamma_P(r)]$ data set to Eqs. (8a) and (8b). However, inspection of Eqs. (6a)–(6c) reveals that evaluation of the two activity coefficients depends upon the assignment of a value of $c_A(r)$ for each $\bar{c}(r)$ throughout the distribution. This difficulty is readily overcome by adopting an iterative approach with an initial estimate of the composition distribution based on assumed thermodynamic ideality.

3. Methods

The effectiveness of the SPT approach to the characterization of nonideal protein self-association is to be examined by analyzing sedimentation equilibrium distributions that have been simulated for monomer–tetramer systems involving a 66 kDa monomer with a net charge of −20. Although these values of M_A and Z_A have been selected to emulate a protein such as serum albumin at neutral pH, the resulting analysis would also apply at a pH where the net charge was correspondingly positive because of the description of electrostatic repulsion involves the product of charges (either Z_A^2 or Z_AZ_P with both bearing the same sign). On the grounds that the assignment of magnitudes to activity coefficients via Eqs. (2a) and (2b) is a prerequisite for simulating sedimentation equilibrium distributions, this aspect is considered first.

As noted in the previous section, values of the three virial coefficients required for the calculation of activity coefficients (B_{AA}, B_{PP}, B_{AP}) have been obtained by means of Eqs. (4a)–(4c). The numerical integrations inherent therein have entailed the substitution of a distance increment (Δx) of 0.02 nm for dx and the choice of an upper-limiting value of x for the summation that sufficed to render negligible the contributions of additional terms in the indefinite summation. For these calculations the monomer was assigned a radius (R_A) of 3.5 nm, and that of tetramer (R_P) was taken as 5.83 nm — a value about 5% greater than that of 5.56 nm deduced on the basis of spherical geometry for both species ($R_P = n^{1/3}R_A$). In similar vein the tetramer has been assigned a net charge of −76 rather than −80 to accommodate probable lack of charge conservation in the association of monomer with an assigned net charge of −20. Incorporating these departures from strict conformity with the potential-of-mean-force (PMF) model in the simulated distributions should provide some indication of the likely consequences of employing the PMF model to analyze sedimentation equilibrium distributions obtained experimentally for a self-associating protein bearing net charge.

The simulation of sedimentation equilibrium distributions at 293 K and 15,000 rpm was initiated by assigning a value of 1.500 g/L to the thermodynamic activity of monomer, $M_Az_A(r_F)$, at a reference radial distance r_F in a liquid column spanning the radial distance range 6.850–7.150 cm. After calculation of the monomer thermodynamic activity $M_Az_A(r)$ at 0.002 cm intervals (Δr) throughout the column by means of Eq. (7) for the 66 kDa monomer with $\bar{\nu}\rho_s$ taken as 0.74, Eq. (1b) was used to generate the corresponding distribution of tetramer thermodynamic activity, $M_Pz_P(r)$ for a range of values of the association constant X_4. By considering these values of $M_Az_A(r)$ and $M_Pz_P(r)$ to be initial estimates of $c_A(r)$ and $c_P(r)$ respectively, values of the corresponding activity coefficients, $\gamma_A(r)$ and $\gamma_P(r)$ were calculated from Eqs. (2a) and (2b). Recalculation of $c_A(r)$ and $c_P(r)$ on the basis of those activity coefficient estimates then allowed refinement of the activity coefficient values; and this cycle was repeated until no further change occurred in the estimates of $c_A(r)$ and $c_P(r)$. The total protein concentration distribution, $\bar{c}(r)$ as a function of r, was then taken as the sum of these final estimates of $c_A(r)$ and $c_P(r)$. These simulated sedimentation distributions with an upper concentration limit of 8–10 mg/mL were then converted to Rayleigh fringe counterparts on the basis of 3.33 fringes for 1 mg/mL protein [26], after which random error with a standard deviation of 0.02 fringes [27] was superimposed on the fringe distribution.

Analysis of these simulated distributions by the SPT method [11,13–15,17] also entailed an iterative approach. The first fitting of a distribution to Eqs. (8a) and (8b) was conducted with values of unity for both activity coefficients to obtain an initial estimate of $M_Az_A(r_F)$ and hence $M_Az_A(r)$ throughout the distribution via Eq. (7). Substitution of the consequent values of $M_Az_A(r)$ for $c_A(r)$ and $[\bar{c}(r) - c_A(r)]$ for $c_P(r)$ into Eqs. (6a)–(6c) then provided initial estimates of $\gamma_A(r)$ and $\gamma_P(r)$ throughout the sedimentation equilibrium distribution. Nonlinear regression of the revised data set $[\psi_A(r), \bar{c}(r), \gamma_A(r), \gamma_P(r)]$ in terms of Eqs. (8a) and (8b) then led to improved estimates of $M_Az_A(r_F)$ and hence $c_A(r) = M_Az_A(r_F)\psi_A(r)/\gamma_A(r)$, thereby allowing refinement of the composition and hence activity coefficients. This iterative process was continued until essentially no further change (<0.002) occurred in the returned values of $\gamma_A(r)$ and $\gamma_P(r)$ for the highest concentrations. Because this requirement proved to be more stringent than constancy of $M_Az_A(r_F)$, the value of X_n returned as the other curve-fitting parameter was then taken as the best estimate of the thermodynamic association constant for reversible self-association of the protein. As in our previous investigation [1], activity coefficients pertaining to each concentration $\bar{c}(r)$ throughout a distribution were obtained by means of an Excel spreadsheet and then pasted into the SCIENTIST package (Micromath Scientific Software, Salt Lake City, UT) for nonlinear least-squares curve-fitting to Eqs. (8a) and (8b) for the determination of the best-fit values of X_4 and $M_Az_A(r_F)$.

The simulated sedimentation equilibrium distributions were also analyzed by the potential-of-mean-force method to ascertain the feasibility of determining the monomer charge (Z_A) as well as the tetramerization constant on the basis of the sum-of-squares-of-residuals (SSR) associated with best-fit descriptions obtained by nonlinear least-squares curve-fitting to Eqs. (8a) and (8b). Specifically, the curve-fitting to Eqs. (8a) and (8b) was preceded by iterative deduction of the required activity coefficients $[\gamma_A(r), \gamma_P(r)]$ from second virial coefficients obtained by numerical integration [Eqs. (4a)–(4c) and (5a)–(5b)] for a range of assigned values of Z_A using the values of R_P (5.56 nm) and Z_P (−80) based on spherical geometry and charge conservation.

4. Results and discussion

As illustrated previously [1], the use of scaled particle theory for the characterization of nonideal self-association [11,13–15] is equivalent to use of the McMillan–Mayer treatment of non-ideality on the basis of the potential-of-mean-force between uncharged particles [18]. For charged species, however, the only course of action available in the SPT approach is to increase the effective size of the particle to account for the additional non-ideality arising from electrostatic repulsion [12,16]. This additional non-ideality is accommodated quantitatively by the potential-of-mean-force method for the special situation in which the net charge is spread uniformly over the spherical particle. Although this model represents an oversimplified description of an actual protein, the adequacy of its use for thermodynamic purposes has been demonstrated in physicochemical studies of ovalbumin which have yielded close correspondence between observed non-ideality and that predicted on the basis of the covolume radius obtained under isoelectric conditions and experimental estimates of the net charge ([28–30]). Sedimentation equilibrium distributions simulated on the basis of virial coefficients obtained by the potential-of-mean-force model are therefore considered to be adequate for the current test of the efficacy of the SPT approach to characterizing self-association of charged proteins, In that regard the assignment of appropriate magnitudes to the various second virial coefficients is clearly crucial to the exercise.

4.1. Magnitudes of second virial coefficients

In most sedimentation equilibrium studies thus far reported the second virial coefficients B_{ii} and B_{ij} have been calculated from the first two terms of Eq. (3). The need for extension of these expressions was recognized by the existence of discrepancies between such estimates and those obtained by numerical integration [Eqs. (4a)–(4c) and (5a)–(5b)] in an investigation of α-chymotrypsin dimerization at low ionic strength [5]. Although inclusion of the final terms in Eq. (3) to calculate the virial coefficients has potential to provide better estimates (21), Eqs. (4a)–(4c) and (5a)–(5b) with their inherent requirements for numerical integration have been used for all calculations of virial coefficients because of the large magnitude of Z_P for the tetramer species.

The necessity for so doing is emphasized by the virial coefficients reported in Table 1, where the values obtained by numerical integration are followed in parentheses by the respective estimates obtained from the truncated and complete versions of the approximate solution [Eq. (3)]. Only for monomer self-interaction at physiological ionic strength ($I_M = 0.15$ M) can the approximate values be regarded as acceptable estimates of the second virial coefficient (B_{AA}) for this system involving a monomer with the size and charge characteristics of serum albumin. Although the series in the approximate solution is converging for both B_{PP} and B_{AP} at the higher ionic strength, the convergence is too slow for the approximate solution to be a viable option because of the large charge (−40) on the tetramer. At the lower ionic strength ($I_M = 0.05$ M), chosen to enhance the influence of electrostatic repulsion on the magnitudes of second virial coefficients, the approximate solutions do not even provide an acceptable estimate of B_{AA}, their use for estimating B_{PP} and B_{AP} being precluded altogether by divergence of the series in Eq. (3). These observations reinforce a previous assertion [21] of the need to exercise caution in the use of approximate solutions for the potential-of-mean-force for proteins bearing sizeable net charge.

4.2. Analysis of simulated sedimentation equilibrium distributions by the potential-of-mean-force method

As noted in the Methods section, sedimentation equilibrium distributions have been simulated at a rotor speed (15,000 rpm) selected to yield concentration (Rayleigh fringe) data with a lower limit of about 0.25 mg/mL and an upper limit of 8–9 mg/mL. In practice the characterization of protein self-association would entail sedimentation equilibrium experiments with a range of loading concentrations conducted at several speeds. However, a simulated run approaching high-speed design [31] suffices to test the likely efficacy of the SPT analysis because it effectively spans the entire range (0–10 mg/mL) for which effects of thermodynamic non-ideality are in practice routinely restricted to the consequences of nearest-neighbor interactions and hence to description solely in terms of second virial coefficient terms.

Because of the involvement of Eqs. (4a)–(4c), (5a)–(5b), and (8a)–(8b) in generation of the simulated sedimentation equilibrium distributions, their use for the analysis of those distributions should obviously lead to acceptable estimates of the input tetramerization constants. In that regard such nonlinear least-squares curve-fitting of distributions to Eqs. (8a) and (8b) with magnitudes of second virial coefficients and hence activity coefficients based on $Z_A = 20$ leads to estimates of X_4 that are 96–98% of input values. The small disparity between X_4^{est} and X_4 presumably reflects error arising from minor differences between the relationships $R_P = 4^{1/3}R_A$ and $Z_P = 4Z_A$ incorporated into the PMF analyses of data and those upon which the sedimentation equilibrium distributions were simulated (Table 1).

A limitation of the potential-of-mean-force method is its requirement for the assignment of absolute magnitudes to Z_A and Z_P, the respective net charges of the monomer and polymer species. On the grounds that protein charge is a fundamental but elusive parameter that is seldom measured [32–34], we have repeated the above analyses for a range of Z_A and Z_P (taken as $4Z_A$) values to ascertain whether an appropriate value of monomer charge can be identified on the basis of a minimum in the sum-of-squares-of-residuals (SSR) for the best-fit descriptions. Fig. 1A presents the sedimentation equilibrium distribution (♦) simulated for the system with highest association constant ($X_4 = 0.000278$ L^3 g^{-3}, I_M 0.15 M) as well as the best-fit description (——) obtained with monomer valence set at −18.7, the value of Z_A^{est} corresponding to the minimum in the SSR of best-fit descriptions for Z_A^{est} between −18 and −22. Also shown is the residuals plot (▲), in which the maximum disparity is 1% of the value. From Fig. 1B it is evident that reasonable agreement is also observed between the concentration dependencies of the simulated activity coefficients (——) and those (♦) deduced as part of the iterative curve-fitting process. Those dependencies virtually superimpose for the activity coefficient of monomer [$\gamma_A(r)$], but diverge to the extent of 0.04 or 3% (1.44 cf 1.48) for tetramer at the highest protein concentration. That this divergence reflects in part the use of an underestimate for anionic charge ($Z_A = -18.7$ cf −20) is clear from the open symbols in Fig. 1B, which are the activity coefficients associated with the best-fit description of the simulated system for $Z_A^{est} = -20$. Although undesirable, the relatively small disparity in $\gamma_P(r)$ should not affect unduly the concomitantly assessed association constant for the monomer–tetramer system.

Values of Z_A^{est} as well as the corresponding estimates of the association constant and reference thermodynamic activity of monomer are summarized in Table 2, which includes results from potential-of-mean-force analyses on all simulated sedimentation equilibrium distributions. An encouraging finding is the return of estimated association constants that essentially duplicate those obtained by incorporating the net charge of monomer ($Z_A = -20$) into the PMF analysis—a consequence of the fact that the maximum difference between Z_A (−20) and Z_A^{est} is only 2.5%. This observation can be rationalized in two ways. First, the results can be taken to justify use of the PMF approach to obtain estimates of monomer net charge as well as the association constant under conditions where considerations of nearest-neighbor interactions suffice to describe non-ideality in self-association of a protein bearing net charge. Alternatively, they signify that uncertainty about the exact magnitude of Z_A in conventional PMF analyses [4–8] is not likely to have a marked effect on the magnitude of the association constant estimated on the basis of an assigned monomer valence. The calculation of net charge from amino acid sequence data (which takes no account of small-ion binding) is thus likely to provide a satisfactory estimate of Z_A for use in PMF analysis of protein self-association by sedimentation equilibrium—a pleasing outcome in view of the difficulties encountered in experimental determination of protein net charge [32–34].

Table 1
Magnitudes of second virial coefficients for the monomer–tetramer system based on a monomer with characteristics approximating those of serum albumin at neutral pH[a].

Parameter	Calculated value (L/mol)	
	$I_M = 0.15$ M	$I_M = 0.05$ M
B_{AA}	603 (655, 586)[b]	1020 (1400, 750)
B_{PP}	3010 (4160, 360)	4890 (12,000, −16,100)
B_{AP}	2950 (3470, 2640)	4880 (8400, −110)

[a] Values refer to a 66 kDa monomer (A) with $R_A = 3.50$ nm and $Z_A = -20$, and a 264 kDa tetramer with $R_P = 5.83$ nm and $Z_P = -76$.
[b] Numbers in parentheses denote values based on truncated and complete versions of Eq. (3a) for B_{AA} and B_{PP} and Eq. (3b) for B_{AP}.

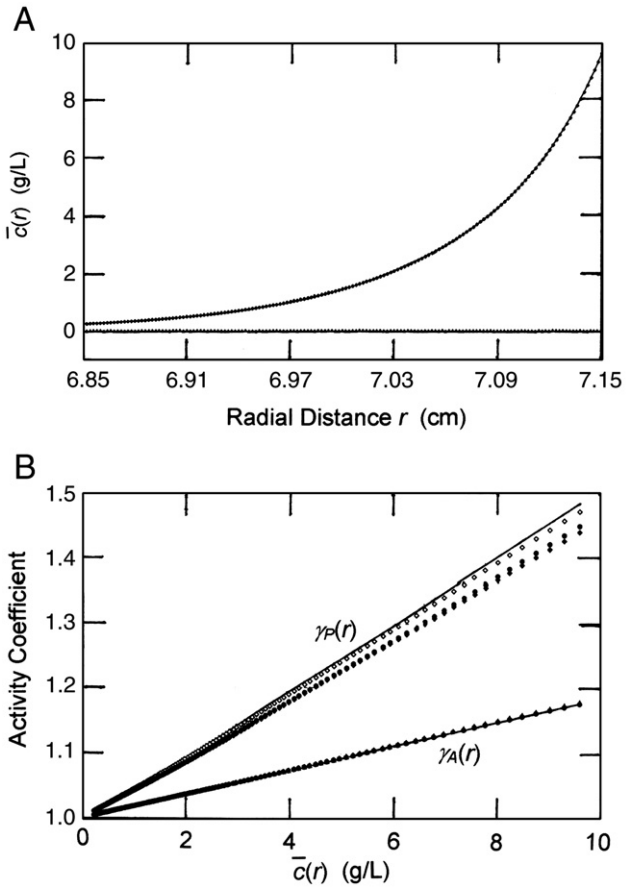

Fig. 1. Analyses of simulated sedimentation equilibrium distributions ($I_M = 0.15$ M) for a monomer–tetramer system with $X_4 = 0.000278$ L^3 g^{-3}. (A) Best-fit description (——) of the simulated data (♦) according to Eqs. (8a) and (8b) with magnitudes of second virial coefficients [Eqs. (4a), (4b), (5b)] and hence activity coefficients [Eqs. (2a), (2b)] based on a monomer valence (Z_A) of −18.7, the value associated with the minimum in SSR of the nonlinear least-squares curve-fitting to Eqs. (8a) and (8b): ▲, plot of residuals. (B) Comparisons of the concentration dependencies of activity coefficients emanating from the analyses with those (——) employed in simulation of the data. ◊, ♦, values obtained by PMF analysis with respective values of −20 and −18.7 for monomer valence (Z_A): ●, corresponding values obtained by the basis of SPT estimates [Eqs. (6a)–(6c)] of activity coefficients for a monomer with $V_A/M_A = 2.17$ mL/g, the value associated with the minimum in SSR of the nonlinear least-squares curve-fitting to Eqs. (8a) and (8b).

Table 2
Summary of analyses designed to evaluate monomer charge as well as the association constant from simulated sedimentation equilibrium distributions on the statistical–mechanical basis of the potential-of-mean-force between molecules.

$10^4 X_4$ (L^3 g^{-3})	Z_A^{est} [a]	$z_A(r_F)$ (mg mL^{-1}) [b]	$10^4 X_4^{est}$ (L^3 g^{-3})	(X_4^{est}/X_4)	$(X_4^{est}/X_4)_{Z_A=20}$
Ionic strength 0.15 M					
2.78	18.7	1.4988 (±0.0008) [c]	2.65 (±0.02) [c]	0.95	0.97
2.23	20.3	1.5012 (±0.0008)	2.17 (±0.02)	0.96	0.97
1.67	19.3	1.4999 (±0.0008)	1.60 (±0.02)	0.96	0.97
1.11	20.5	1.5014 (±0.0008)	1.11 (±0.02)	1.00	0.99
0.56	19.9	1.4994 (±0.0007)	0.55 (±0.02)	0.98	0.98
Ionic strength 0.05 M					
2.78	19.6	1.4988 (±0.0009)	2.67 (±0.02)	0.96	0.97
2.23	19.5	1.4973 (±0.0008)	2.12 (±0.02)	0.95	0.97
1.67	19.7	1.4911 (±0.0009)	1.60 (±0.02)	0.96	0.97
1.11	19.8	1.4999 (±0.0008)	1.06 (±0.02)	0.95	0.97
0.56	19.9	1.5004 (±0.0008)	0.53 (±0.02)	0.95	0.96

[a] Absolute value of monomer charge associated with the minimum in SSR.
[b] Input value of 1.5000 mg/mL used in the simulations.
[c] Numbers in parentheses denote the uncertainty (±2 SD) of the estimate.

4.3. SPT analysis of simulated sedimentation equilibrium distributions

If the monomer under consideration were non-interacting the effects of thermodynamic non-ideality in a solution of *A* alone would be described by the relationship $C_A d\ln\gamma_A / dC_A = 2B_{AA}C_A$. In that regard it is immaterial whether the value of 603 L/mol for B_{AA} at $I_M = 0.15$ M (Table 1) is regarded as reflecting a species with volume $V_A = 4\pi LR_A^3/3$ of 108 L/mol and a net charge of −20 (the potential-of-mean-force model), or as an uncharged species with an effective volume $V_A^{eff} = B_{AA}/4$ of 151 L/mol (the SPT model). Adoption of this SPT approach at the lower ionic strength (0.05 M) necessitates revision of V_A^{eff} to 255 L/mol. Similarly, for a solution of non-interacting tetramer the value of 2950 L/mol for B_{PP} at $I_M = 0.15$ (Table 1) can be described in terms of a volume $V_P = 4\pi LR_P^3/3$of 500 L/mol and a net charge of −76, or as an uncharged species with an effective volume of 738 L/mol: the corresponding value is 1220 L/mol at the lower ionic strength ($I_M = 0.05$ M). In view of the demonstration [1] that the potential-of-mean-force and SPT approaches yield identical values of γ_A and γ_P for mixtures of uncharged spherical particles, the use of these effective volumes (V_A^{eff}, V_P^{eff}) necessarily describes the thermodynamic non-ideality in mixtures of the two species. Indeed, such use of scaled particle theory to describe the thermodynamic non-ideality of inert mixtures has been illustrated experimentally [16,17]; and the same situation should also apply to an interacting mixture of two species (*A* and *P*). However, calculation of the above values of V_A^{eff} and V_P^{eff} implies the availability of magnitudes for R_A, R_P, Z_A and Z_P (or independent estimates of B_{AA} and B_{PP}). On the grounds that the goal of the SPT approach has been avoidance of the need for such detailed specification of the model, we now examine the effectiveness of the two approaches that have been adopted in experimental applications of scaled particle theory to the characterization of nonideal protein self-association by sedimentation equilibrium [13–15].

The simpler approach [13,15] involves the assumption that $V_P^{eff} = nV_A^{eff}$ (i.e., that $x^3 = 1$), whereupon the analysis entails nonlinear least-squares curve-fitting of the $[r, \bar{c}(r)]$ data set to Eqs. (6a)–(6c) and (8a)–(8b) for a range of V_A^{eff}/M_A values to obtain a best-fit estimate of the effective specific monomer volume as that associated with the minimum in the sum-of-squares-of-residuals, whereupon the corresponding values of X_4 and $z_A(r_F)$ are taken as the estimates of the other curve-fitting parameters: activity coefficients deduced in the course of the analysis (●, Fig. 1B) again exhibit reasonable agreement with those used for the simulation. The results of that three-parameter curve-fitting approach are summarized in the upper section of Table 3, from which the values of the reference monomer activity (all within the range $1.497 \le z_A(r_F) \le 1.501$ g/L) have been omitted as a space-saving measure. From a practical viewpoint the agreement between returned estimates and input values of the association constant is a pleasing outcome in that the maximum error in the estimate based on SPT for uncharged spherical particles is only 9%. In the context of reaction energetics that maximum discrepancy between returned and input association constants for the system with $X_4 = 0.000056$ L^3 g^{-3} and $I_M = 0.05$ M translates into a difference of only 0.2 kJ/mol in a standard free energy change (ΔG^0) of −54 kJ/mol for solute self-association.

In the other SPT approach [14] the restrictive requirement that $V_P^{eff} = nV_A^{eff}$ is removed by regarding x^3 as an additional curve-fitting parameter. This approach begins in the same way as that just described in that nonlinear least-squares curve-fitting of the $[r, \bar{c}(r)]$ data set is used to locate the best-fit estimate of V_A^{eff}/M_A for the fixed x^3 value of unity. The effective monomer specific volume is then fixed at that value whilst x^3 is floated to obtain a revised estimate on the basis of a new minimum in the sum-of-squares-of-residuals. Iterative application of those two curve-fitting steps then leads to an overall minimum in the sum-of-squares-of-residuals, whereupon the associated values of V_A^{eff}/M_A, x^3, $z_A(r_F)$ and X_4 are taken as global best-fit

Table 3
Summary of SPT analyses of simulated sedimentation equilibrium distributions reflecting nonideal tetramerization ($4A \leftrightharpoons P$).

$10^4\,X_4$ ($L^3\,g^{-3}$)	Ionic strength 0.15 M				Ionic strength 0.05 M			
	$10^4 X_4^{est}$	X_4^{est}/X_4	V_A^{eff}/M_A[a]	x^3	$10^4 X_4^{est}$	X_4^{est}/X_4	V_A^{eff}/M_A[a]	x^3
Association constant and V_A^{eff}/M_A as curve-fitting parameters								
2.78	2.63[b]	0.95	2.17	1.00[c]	2.73[b]	0.98	3.70	1.00[c]
2.23	2.17	0.97	2.25	1.00	2.21	0.99	3.70	1.00
1.67	1.60	0.96	2.20	1.00	1.67	1.00	3.70	1.00
1.11	1.13	1.02	2.26	1.00	1.14	1.01	3.71	1.00
0.56	0.57	1.02	2.23	1.00	0.61	1.09	3.72	1.00
Association constant, V_A^{eff}/M_A and x^3 as curve-fitting parameters								
2.78	2.63	0.95	2.17	1.01	2.70	0.97	3.69	0.98
2.23	2.18	0.97	2.25	1.01	2.13	0.96	3.68	0.95
1.67	1.61	0.96	2.20	1.01	1.61	0.96	3.69	0.94
1.11	1.01	0.91	2.22	0.69	1.09	0.98	3.70	0.91
0.56	0.61	1.09	2.24	1.18	–	–	–	–

[a] Effective specific volume of monomer (mL/g).
[b] Uncertainty of $0.02\times10^{-4}\,L^3\,g^{-3}$ (±2 SD) in all estimates of the association constant.
[c] Taken as unity in this version of the analysis.

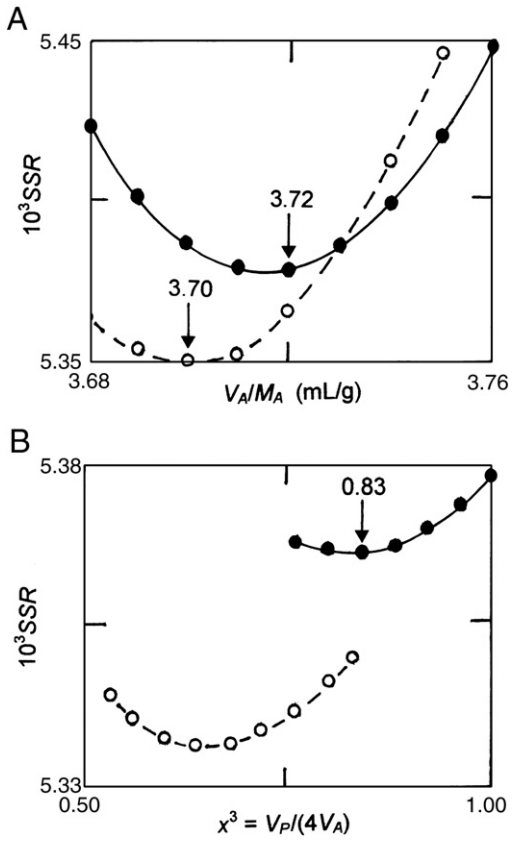

Fig. 2. Attempted location of a global SPT best-fit [minimum in the sum-of-squares-of-residuals (*SSR*)] in nonlinear least-squares curve-fitting of the simulated sedimentation equilibrium distribution with $X_4 = 0.000056\,L^3\,g^{-3}$ at the lower ionic strength ($I_M = 0.05$ M) by alternate fixing of the polymer/monomer volume factor (x^3) and the monomer specific volume (V_A/M_A). (A) Analyses in terms of Eqs. (6a)–(6c) and Eqs. (8a)–(8b) to obtain best-fit estimates of V_A/M_A with x^3 fixed initially at unity (●) and then 0.83 (○) (see B). (B) Subsequent estimations of the best-fit values of x^3 for fixed monomer specific volumes of 3.72 (●) and 3.70 (○) mL/g (see A).

estimates. Results of those analyses of nine of the simulated sedimentation equilibrium distributions are summarized in the lower section of Table 3, the unreported reference monomer activities all being within the range $1.496 \le z_A(r_F) \le 1.501$ g/L.

In most instances this removal of the inflexible and incorrect relationship between V_A^{eff} and V_P^{eff} inherent in the simpler SPT model has had little effect on the estimates of the association constant, which remain within 9% of the input values. However, a potential problem with this approach is signified by the lack of entries in Table 3 for the most weakly associating system at the lower ionic strength. As already signified in the upper part of Table 3, the initial analysis with $x^3 = 1$ leads to a reasonable estimate (within 9%) of X_4 and the value of 3.72 mL/g for V_A^{eff}/M_A that is associated with the minimum in the sum-of-squares-of-residuals (●, Fig. 2A). In contrast with the behavior observed for most of the other systems, the second stage of the analysis with V_A^{eff}/M_A fixed reveals (●, Fig. 2B) that a pronounced improvement in fit can be effected by lowering x^3 substantially (a minimum in SSR at $x^3 = 0.83$). Furthermore a similar lowering of the SSR occurs during the next round of analyses (○, Fig. 2B) with the effective monomer specific volume fixed at 3.70 mL/g, the best-fit estimate for $x^3 = 0.83$ (○, Fig. 2A). From a statistical viewpoint the analysis should obviously be continued to find values of x^3, V_A^{eff}/M_A, z_A (r_F) and X_4 associated with a global minimum in SSR; but the analysis was discontinued because the current estimate of 0.65 for x^3 was already untenable on the physical grounds that unity is a realistic lower-limiting value for this relative size parameter [$x^3 = V_P^{eff}/(nV_A^{eff})$]. Despite the fact that rigid application of the criterion that x^3 should be greater than unity would lead to rejection of most of the analyses reported in the lower part of Table 3, the associated values of X_4 are eminently reasonable—even for the system with an estimate of 0.69 for x^3. Although a seemingly unreasonable value for x^3, or its relative radius counterpart (r_P/r_A), has been used in the past as sufficient reason for rejecting modes of solute self-association [15], such action is not necessarily justified. On the grounds that the introduction of this additional parameter has led to no substantial improvement in estimates of the tetramerization constants (Table 3), there is little to be gained by extending the SPT analysis beyond the standard analysis with $x^3 = 1$.

These applications of scaled particle theory for characterizing nonideal self-association from simulated sedimentation equilibrium distributions for charged protein systems have thus established its likely adequacy as a procedure for determining the association constant for a specified stoichiometry of reaction. However, despite the observation of reasonable agreement between estimated and input values of the tetramerization constant for most systems (Table 3), the two size-related quantities [V_A^{eff}/M_A and $x^3 = V_P^{eff}/(nV_A^{eff})$] are merely empirical curve-fitting parameters that may bear little relationship to the physical characteristics of the species that they supposedly characterize. As noted above, that observation certainly renders open to question the practice [14] of using the magnitudes of these curve-fitting parameters as a criterion for assessing the credibility of the characterization for a specified stoichiometry of self-association—a criterion that was in fact applied uncritically. For ribonuclease (Table 1 of [14]) a monomer–dimer model of self-association is rejected on the physical grounds of an unrealistic ratio (0.83) for R_P/R_A (or 0.29 for x^3). On the other hand a monomer–trimer model is deemed acceptable despite the return of a value of 0.75 for x^3. A similar inconsistency is observed for ovalbumin (Table 2 of [14]), where interpretation of data in terms of a monomer–tetramer model is regarded as acceptable despite the return of a value of 0.72 for x^3. In the light of present findings it is questionable whether any of the analyses presented in Tables 1 and 2 of [14] can be rejected on physical grounds because x^3 (or R_P/R_A) is now seen to be merely a curve-fitting parameter that may bear little relationship to the physical parameter that it purportedly represents. In that regard the reversion to the simpler approach ($x^3 = 1$) in a subsequent SPT analysis of nonideal protein self-association [15] may well signify that the Minton group has also reached this conclusion.

5. Concluding remarks

This theoretical investigation has explored two statistical–mechanical approaches to characterize the nonideal self-association of a protein bearing net charge under conditions where consideration of nearest-neighbor interactions suffices to describe effects of thermodynamic non-ideality. In one of those methods [11,13–16] the inability of scaled particle theory to incorporate specific allowance for the effects of solute charge has necessitated the introduction of effective volume parameters (V_A^{eff}, x^3) to accommodate the additional thermodynamic non-ideality arising from the existence of charge on the protein molecules. In the approach based on the potential-of-mean-force between charged molecules [4–8,13–16], specific account is taken of the non-ideality contribution arising from electrostatic repulsion between like-charged species, but only in situations where the net charge is spread uniformly over the species. The current use of this model as a basis for simulating thermodynamically nonideal sedimentation equilibrium distributions is open to criticism because of that restrictive condition; but its use reflects the absence of a more realistic theoretical description of thermodynamic non-ideality in charged systems that find ready application.

A pleasing outcome of this investigation has been the support provided for the validity of scaled-particle-theory analyses from the viewpoint of determining the self-association constant for a specified reaction stoichiometry under conditions where consideration of nearest-neighbor interactions suffices to describe effects of thermodynamic non-ideality. However, the practice of distinguishing between different modes of self-association by assigning physical significance to the magnitudes of the effective size parameter(s) is rendered rather tenuous by present findings.

These observations reinforce the desirability of expanding an experimental investigation to incorporate the measurement of quantities such as size and charge of the solvated monomer in order to decrease the number of parameters being deduced by nonlinear least-squares curve-fitting, and thereby to obtain a more definitive characterization of the self-association of a charged protein system by direct analysis of sedimentation equilibrium distributions. In that regard, it would appear that consideration of monomer net charge as an additional parameter to be evaluated by PMF analysis can obviate to some extent the problems of experimental net charge determination. At this stage an important aspect requiring further investigation is the adequacy of the widespread practice of restricting considerations of thermodynamic non-ideality to effects of nearest-neighbor interactions, an assumption upon which the present conclusions are, of course, reliant.

Glossary of symbols

B_{ij}	second virial coefficient for physical interaction between species i and j
C_i	molar concentration of species i
K_n	molar association constant for the reaction $nA \leftrightarrows C$
M_A	molar mass of monomer
R_i	molecular radius of species i
V_A^{eff}	effective molar volume of monomer (scaled particle theory)
X_n	equilibrium constant for self-association expressed on a weight concentration scale
Z_i	net charge (valence) of species i
c_i	weight concentration of species i
r	radial distance
$\bar{\nu}_i$	partial specific volume of species i
z_i	molar thermodynamic activity of species i
$z_i(r)$	thermodynamic activity of species i at radial distance r [Eq. (7)]
$\gamma_i(r)$	molar activity coefficient of species i
κ	Debye inverse screening length
ω	angular velocity of centrifugation
$\psi_i(r)$	normalized radial distance in sedimentation equilibrium [Eq. (8b)].

Acknowledgements

PRW thanks the University of Auckland for office, computing and library facilities. DJS was supported by a grant (ref: BBF0111561) from the Biotechnology and Biological Sciences Research Council (UK).

References

[1] D.J. Scott, D.J. Winzor, Comparison of methods for characterizing nonideal solute self-association by sedimentation equilibrium, Biophys. J. 97 (2009) 886–896.
[2] E.T. Adams, H. Fujita, Sedimentation equilibrium in interacting systems, in: J.W. Williams (Ed.), Ultracentrifugation in Theory and Experiment, New York, Academic Press, 1963, pp. 119–128.
[3] T.L. Hill, Y.D. Chen, Theory of aggregation in solution. 1. General equations and application to the stacking of bases, nucleosides, etc. Biopolymers 12 (1973) 1285–1312.
[4] P.R. Wills, M.P. Jacobsen, D.J. Winzor, Direct analysis of solute self-association by sedimentation equilibrium, Biopolymers 38 (1996) 119–130.
[5] P.R. Wills, D.J. Winzor, Studies of solute self-association by sedimentation equilibrium: allowance for effects of thermodynamic nonideality beyond the consequences of nearest-neighbor interactions, Biophys. Chem. 91 (2001) 253–262.
[6] P.R. Wills, D.J. Winzor, Allowance for thermodynamic nonideality in sedimentation equilibrium, in: D.J. Scott, S.E. Harding, A.J. Rowe (Eds.), Modern Analytical Ultracentrifugation: Techniques and Methods, Royal Society of Chemistry, Cambridge, UK, 2005, pp. 64–103.
[7] P.R. Wills, L.W. Nichol, R.J. Siezen, The indefinite self-association of lysozyme: consideration of composition-dependent activity coefficients, Biophys. Chem. 11 (1980) 71–82.
[8] M.P. Jacobsen, D.J. Winzor, Refinement of the omega analysis for the quantitative characterization of solute self-association by sedimentation equilibrium, Biophys. Chem. 45 (1992) 119–132.
[9] J.L. Lebowitz, E. Helfand, E. Praestergaard, Scaled particle theory of fluid mixtures, J. Chem. Phys. 43 (1965) 774–779.
[10] R.M. Gibbons, The scaled particle theory for particles of arbitrary shape, Mol. Phys. 17 (1969) 81–86.
[11] R.C. Chatelier, A.P. Minton, Sedimentation equilibrium in macromolecular solutions of arbitrary concentration. 1. Self-associating proteins, Biopolymers 26 (1987) 507–524.
[12] A.P. Minton, H. Edelhoch, Light scattering of bovine serum albumin solutions: extension of the hard particle model to allow for electrostatic repulsion, Biopolymers 21 (1982) 451–458.
[13] N. Muramatsu, A.P. Minton, Hidden self-association of proteins, J. Mol. Recognit. 1 (1989) 166–171.
[14] M. Zorilla, M. Jiménez, P. Lillo, G. Rivas, A.P. Minton, Sedimentation equilibrium in a solution containing an arbitrary number of solute species at arbitrary concentrations: theory and application to concentrated solutions of ribonuclease, Biophys. Chem. 108 (2004) 89–100.
[15] M. Jiménez, G. Rivas, A.P. Minton, Quantitative characterization of weak self-association in concentrated solutions of immunoglobulin G via the measurement of sedimentation equilibrium and osmotic pressure, Biochemistry 46 (2007) 8373–8378.
[16] A.P. Minton, Effective hard particle model for the osmotic pressure of highly concentrated binary solutions, Biophys. J. 94 (2008) L57–L59.
[17] C. Fernández, A.P. Minton, Static light scattering from concentrated protein solutions. II. Experimental test of theory for protein mixtures and weakly self-associating proteins, Biophys. J. 96 (2009) 1992–1998.
[18] W.G. McMillan, J.E. Mayer, The statistical thermodynamics of multicomponent systems, J. Chem. Phys. 13 (1945) 276–305.
[19] T.L. Hill, Theory of solutions. II. Osmotic pressure virial expansion and light scattering in two-component solutions, J. Chem. Phys. 30 (1959) 93–97.
[20] P.R. Wills, D.J. Winzor, Exact theory of sedimentation equilibrium made useful, Prog. Colloid Polym. Sci. 119 (2002) 113–120.
[21] D.J. Winzor, P.R. Wills, Direct allowance for the effects of thermodynamic nonideality in the quantitative characterization of protein self-association by osmometry, Biophys. Chem. 145 (2009) 64–71.
[22] H. Reiss, H.L. Frisch, J.L. Lebowitz, Statistical mechanics of rigid spheres, J. Chem. Phys. 31 (1959) 369–380.
[23] R.H. Haschemayer, W.F. Bowers, Exponential analysis of concentration or concentration difference data for discrete molecular weight distributions in sedimentation equilibrium, Biochemistry 9 (1970) 435–445.
[24] B.K. Milthorpe, P.D. Jeffrey, L.W. Nichol, Direct analysis of sedimentation equilibrium results obtained with polymerizing systems, Biophys. Chem. 3 (1975) 169–175.
[25] P.R. Wills, W.D. Comper, D.J. Winzor, Thermodynamic nonideality in macromolecular solutions: interpretation of virial coefficients, Arch. Biochem. Biophys. 300 (1993) 206–212.
[26] P. Voelker, Measurement of the extinction coefficient of prostate specific antigen using interference and absorbance optics in the Optima-XL-A analytical ultracentrifuge, Prog. Colloid Polym. Sci. 99 (1995) 162–166.

[27] A.J. Rowe, Weak interactions: optical algorithms for their study in the AUC, in: D.J. Scott, S.E. Harding, A.J. Rowe (Eds.), Modern Analytical Ultracentrifugation: Techniques and Methods, Royal Society of Chemistry, Cambridge UK, 2005, pp. 484–500.
[28] R.J. Siezen, L.W. Nichol, D.J. Winzor, Exclusion chromatography of concentrated hemoglobin solutions: comparison of the self-association behavior of the oxy and deoxy forms of the $\alpha_2\beta_2$ species, Biophys. Chem. 14 (1981) 221–231.
[29] P.R. Wills, D.R. Hall, D.J. Winzor, Interpretation of thermodynamic nonideality in sedimentation equilibrium experiments on proteins, Biophys. Chem. 84 (2001) 217–225.
[30] D.J. Winzor, L.E. Carrington, S.E. Harding, Analysis of thermodynamic nonideality in terms of protein solvation, Biophys. Chem. 93 (2001) 231–240.
[31] D.A. Yphantis, Equilibrium ultracentrifugation in dilute solutions, Biochemistry 3 (1964) 297–317.
[32] D.J. Winzor, Determination of the net charge (valence) of a protein: a fundamental but elusive parameter, Anal. Biochem. 325 (2004) 1–20.
[33] D.J. Winzor, L.E. Carrington, S.E. Harding, Limitations of the ultracentrifugal approach for measuring the effective net charge of a macroion, Anal. Biochem. 333 (2004) 114–118.
[34] D.J. Winzor, S. Jones, S.E. Harding, Determination of protein charge by capillary electrophoresis, Anal. Biochem. 333 (2004) 225–229.